

## **Enhancement of Photoconductive Detector Based on Carbon Nanotubes Decorated with Silver Nanoparticles by Adding Conductive Polymer**

**Taqwa Y. Yousif<sup>\*</sup>, Asama N. Naje<sup>a</sup>**

Department of Physics, College of Science, University of Baghdad, Baghdad, Iraq

<sup>a</sup>E-mail: naje.as75@gmail.com

<sup>\*</sup>Corresponding author: ty3033@gmail.com

### **Abstract**

In this work, wide band range photo detector operating in UV, Visible and IR was fabricated using carbon nanotubes (MWCNTs, SWCNTs) decorated with silver nanoparticles (Ag NPs). Silicon was used as a substrate to deposited CNTs/Ag NPs by the drop casting technique. Polyamide nylon polymer was used to coat CNTs/Ag NPs to enhance the photo-response of the detector. The electro-exploding wire technology was used to synthesize Ag NPs. Good dispersion of silver NPs achieved by a simple chemistry process on the surface of CNTs. The optical, structure and electrical characteristic of CNTs decorated with Ag NPs were characterized by X-Ray diffraction and Field Emission Scanning Electron Microscopy. X-ray diffraction patterns of Ag NPs exhibited  $2\theta$  values ( $38.1^\circ, 44.3^\circ$ ) corresponding to the Ag nanocrystal, while the XRD pattern of MWCNTs and SWCNTs /Ag NPs peaks appeared at  $2\theta = 26.2^\circ$  corresponding to the (002) and at  $2\theta = 44^\circ$  which corresponds with miller indices (100) for CNTs and (200) for Ag NPs. The optical properties measured by UV-Vis. Spectroscopy. Broad and strong surface plasmon resonance (SPR) peak was detected at 420 nm, for Ag NPs. The absorption of CNTs/Ag NPs increased significantly from UV to near IR region (300-1000 nm). Ag NPs decorated CNTs without any impurities, according to field mission scanning electron microscopy examination, with typical particle sizes of (50-80nm) for Ag-NPs, 44nm for MWCNTs/Ag-NPs, and 30nm for SWCNTs/Ag NPs. The I-V characteristics at forward bias voltage (0.5-10) volt were studied. The figure of merits (responsivity, photocurrent gain, NEP and detectivity) after coating with polymer of the detector were measured in the dark and after illumination with UV LED (365 nm), Tungsten lamp (500-800 nm) and Laser diode (808 nm).

### **Article Info.**

#### **Keywords:**

*SWCNTs, MWCNTs, Ag NPs, polyamide nylon polymer, Photo conductive detector.*

#### **Article history:**

*Received: Jun. 10, 2021*

*Accepted: Aug. 12, 2021*

*Published: Sep. 01, 2021*

### **1. Introduction**

In the past few years, there had been many significant studies on nano-crystalline materials due to their particular characteristics that bulk materials lack since nanoparticles have an extensive quantity of surface atoms than that of bulk [1]. Carbon nanotubes (SWCNTs & MWCNTs) and metal nanoparticles have various unique properties that make them useful in the field of optoelectronic and nanotechnology applications. CNTs have a wide range of thermal, electrical and structural properties [2, 3] Metal nanoparticles (NPs) have gained interest in the domains of electronics, chemistry, and biology due to their high surface-to-volume ratio and the size effect, which gives nanoparticles distinguishable features (optical, chemical, electrical, and magnetic) from their bulk material [4, 5]. CNTs decorated with metal nanoparticles

open up new possibilities for researchers in a variety of domains, and are likely to have different properties than individual CNTs, such as electrical, magnetic, and optical capabilities [5]. Photodetectors play an important function in many applications of modern life such as thermal imaging, night vision, medical and remote sensing, and chemical testing [6]. Photoconductivity is the most generally used effect in which the radiation incident on material changes to the electrical conductivity [7]. Previous studies focused on the infrared (IR) response of CNTs, which explained that CNTs have possible application in IR detector [8, 9]. To enhance the photo-response of the photoconductive detector, the samples were coated with polyamide nylon polymer.

## 2. Experimental work

### 2.1. Synthesis of Ag-NPs by Electro-Expanding Wire (EEW)

This study developed simple and effective technologies for processing huge quantities of metal nanoparticles for wire explosions. Two electrodes were fixed in a Teflon beaker; two electrodes were fixed in a Teflon beaker as shown Fig.1. Metal plate was fixed on the bottom of the Teflon beaker, while a wire was placed opposite to the metal plate. Thick copper wires were used to connect the positive terminal of the battery 36V DC battery (welding machine) to the metal plate by an ohmic contact. The negative terminal of the battery was connected to the wire to be exploded through another ohmic contact by passing high current about 100A through it. (Fig.1). The Teflon beaker was filled with 30 ml of distilled water, when just touched by silver wire for 15 hits through precise mechanical movement, and then nominated by filtration paper. The silver nanoparticles will be stuck in the solution.

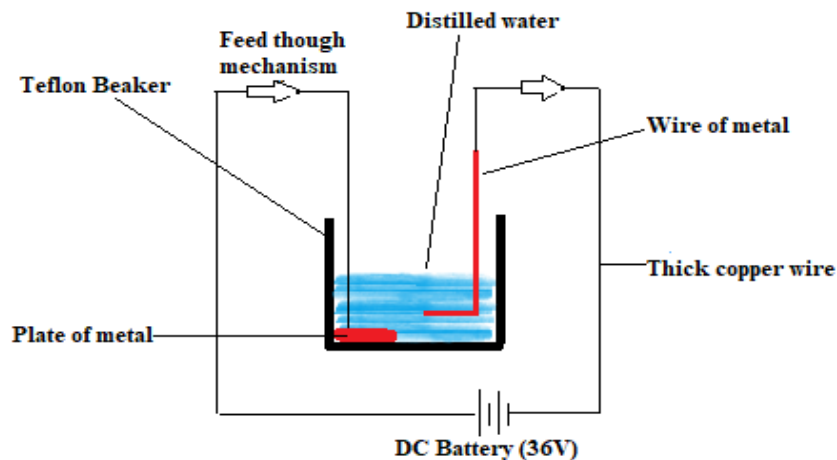


*Figure 1: A schematic diagram for Ag nanoparticles prepared by (EEW) set up.*

Because of the high current density in the wire, the wire explodes in a short amount of time. In the explosion process, silver wires with a purity of 99.99 % and silver plates with (dimension: 2cm<sup>2</sup> area, 0.3mm thickness; purity: 99.99 %) were employed.

### 2.2. Decoration of carbon nanotubes (SWCNT and MWCNT) with Ag NPs

Multi-walled carbon nanotubes (MWCNTs) and single-wall carbon nanotubes (SWCNTs) from (Nanostructured & Amorphous Materials, Inc.) were employed in this study. The diameter of the MWCNTs ranged from 10-30 nm, length 1-2  $\mu\text{m}$  and of 95% purity, and the SWCNTs, its diameter ranged from 1-2 nm, of  $\sim 30 \mu\text{m}$  length and of 90% purity. Decorating CNT (SWCNT & MWCNT) with Ag NPs was carried out by direct mixing. 0.05gm of CNTs (SWCNT & MWCNT) were dissolved in 10ml distilled water, stirred for 1h and sonicated for half hour. 0.5 ml of Ag NPs was added to 2ml of this solution stirred for 12h and sonicated for 1 hour.

### 2.3. Fabrication of photoconductive detector

Si wafer (p-type) of thickness (508±15 μm) and resistivity (1.5 Ω.cm) was used as a substrate of photoconductive detector. The samples of 1.5 x 1.5 cm<sup>2</sup> dimensions were cut from the Si wafer and rinsed in distilled water and ethanol to remove any dirt. Aluminium electrodes, the distance between the two electrodes was 0.4 mm, were made by evaporating Aluminium (Al) under vacuum with the help of a special mask deposited on surface of Si, as shown in (Fig.2).

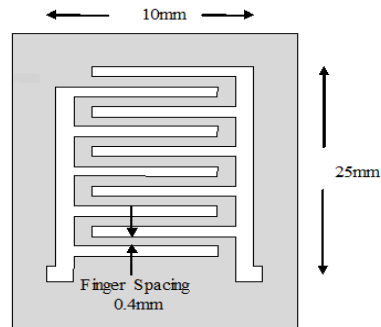


**Figure 2:** Schematic diagram for inter electrodes of photoconductive detector mask.

CNTs/Ag-NPs solution was deposited on the electrodes by drop casting technique, the samples were left aside to dry at room temperature. In order to prepare polyamide nylon polymer solution (0.1 gm) of polyamide nylon polymer was dissolved in 5ml Tetrahydrofuran (THF). The solution was stirred for (10 min) then coated onto the samples by drop casting method. The samples were left in oven to dry. To determine the detector parameters mainly gain, responsivity ( $R_\lambda$ ), specific detectivity ( $D^*$ ) and NEP of the fabricated photoconductive detector on Si substrate by measuring the I-V characteristics, a suitable setup was prepared for this purpose. The system consists of: HUIER DC power supply (ps-1502DD), PC-interfaced digital multimeter (UNI-T UT803). Three sources of light were used for the illumination of the MWCNTs/Ag NPs and SWCNTs/Ag NPs by coating polymer, UV light with wavelength and power (365 nm, 10W) respectively, Tungsten lamp (500-800 nm, 250W) and laser diode (808 nm, 300 mW). The measuring circuit of the I-V characteristics circuit of the photoconductive detector is shown in (Fig.3).

## 3. Results and discussion

### 3.1. UV-Visible absorption spectroscopy

The UV-Visible absorption spectra of the pure Ag-NPs, SWCNT/Ag, and MWCNT/Ag prepared in water media were measured using Shimadzu UV-1800 spectrophotometer. (Fig.4) shows the UV-Visible absorption spectrum of Ag NPs as a function of wavelength. The spectrum reveals that Ag nanoparticles exhibit a fine structural absorption band in the UV-Visible region, with wavelengths ranging from 350 to 750 nanometers. The presence of a broad resonant absorption peak at around 420nm is due to the activation of silver nanoparticles' surface plasmon resonance. According to (Fig.5) MWCNT/Ag and SWCNT/Ag NPs absorb light in the UV, Visible and NIR (300-1000 nm) ranges but the (SPR) peak is smaller than that of the Ag-NPs Because of the induced charge transfer between (SWCNTs and MWCNTs) and Ag NPs, the number of electrons available for surface Plasmon generation in silver nanoparticles could be depleted [10, 11].

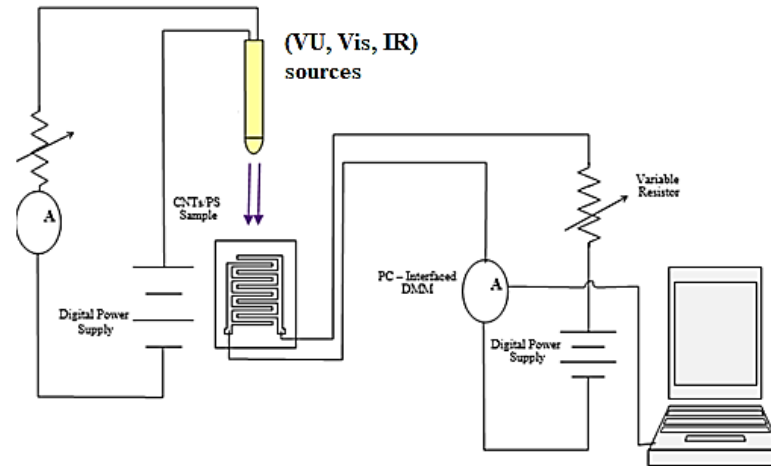


Figure 3: Schematic diagram of the experimental setup of photoconductive detector for I-V characteristics measurements.

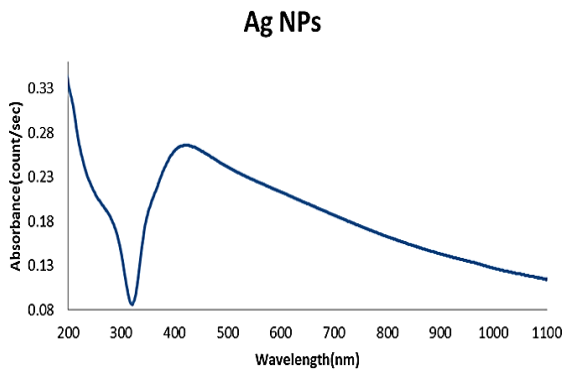


Figure 4: UV-Vis. absorption spectra of Ag nanoparticle.

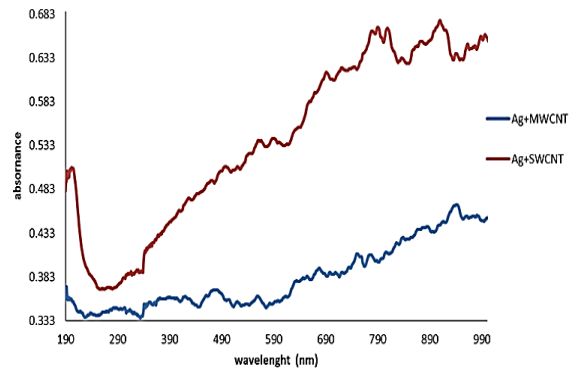


Figure 5: UV-Vis. absorption spectra of SWCNT/Ag & MWCNT/Ag.

### 3.2. Infrared analysis spectroscopy (FTIR)

The functional group of MWCNTs/Ag NPs and SWCNTs/Ag NPs placed on glass substrates was identified using FTIR investigations in the  $400\text{ cm}^{-1}$  to  $4000\text{ cm}^{-1}$  range. Fig. 6 (a and b) shows the FTIR spectra MWCNTs/Ag NPs and SWCNTs/Ag NPs.

To find out how silver nanoparticles interact with carbon nanotubes (SWCNT & MWCNT) molecules. When the FTIR spectra of pure silver nanoparticles and CNTs were compared, it was discovered that the FTIR spectra of SWCNTs/Ag NPs and MWCNTs/Ag NPs contain multiple dips that are also present in the spectrum of pure Ag NPs and CNTs, but with different positions and transmission band intensities. It was slightly shifted to  $(2926, 1752)\text{ cm}^{-1}$ , proving the interaction between the CNTs (SWCNTs & MWCNTs) and Ag nanoparticles molecules. A broad peak appeared at the wavelength of  $(3461\text{ and }3500\text{ cm}^{-1})$  for MWCNTs/Ag NPs and SWCNTs/Ag NPs, respectively which were attributed to O-H stretching vibration. These results are in accordance with reported in the literature [12, 13]. The C=C bonding of aromatic rings of carbon skeleton structure were found at  $1624\text{ cm}^{-1}$ .

### 3.3. X-Ray diffraction

The crystalline structure of Ag nanoparticles, SWCNTs/Ag, and MWCNTs/Ag was studied using X-Ray diffraction. This approach was employed (XRD -6000 labs, supplied by SHIMADZU, with Cu K as the X-ray source), The XRD patterns of silver nanoparticles, MWCNTs/Ag NPs, and SWCNTs/Ag NPs samples are displayed in (Fig.7 (a and b)).

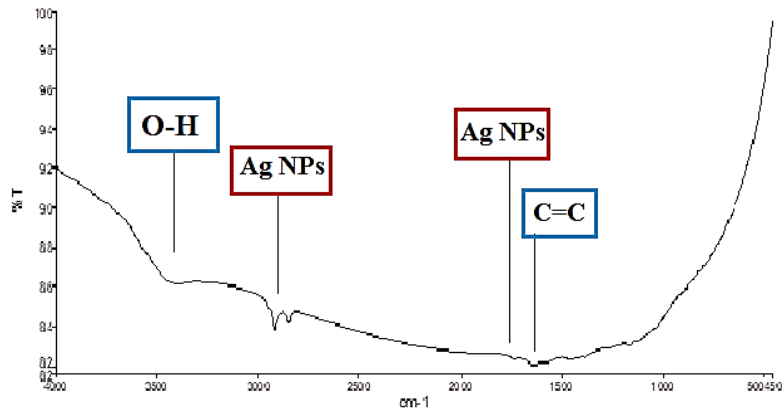


Figure 6a: FTIR spectrum for MWCNTs/Ag NPs thin film.

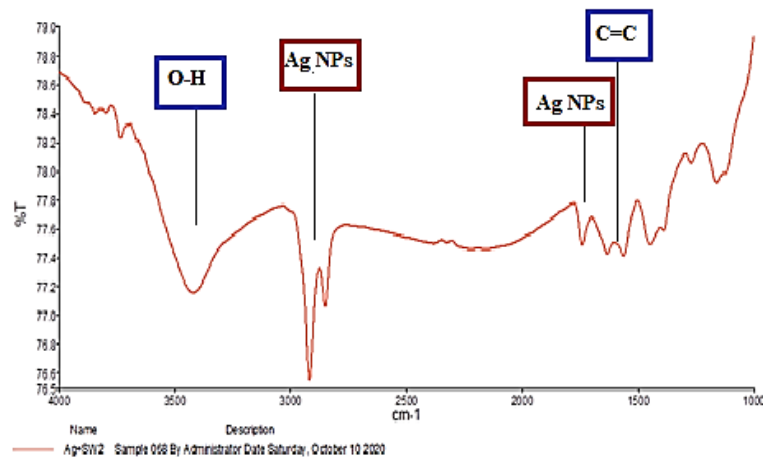


Figure 6b: FTIR spectrum for SWCNTs/Ag NPs thin film.

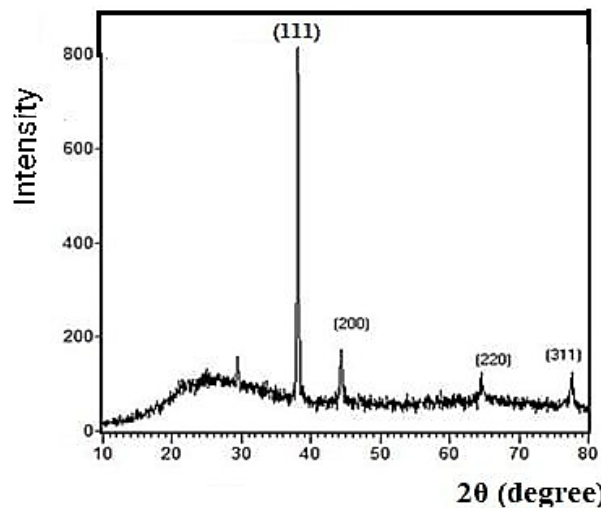


Figure 7a: XRD patterns of pure Ag Nanoparticles thin film.

From Fig.7(a), it can be seen that the pristine Ag-NPs sample exhibits at  $2\theta=38.250^\circ$  corresponding with miller indices (111),  $2\theta=44.353^\circ$  with (200),  $2\theta=64.767^\circ$  with (220) and at  $2\theta=77.604^\circ$  with miller indices (311). The crystalline planes of metallic Ag indicate that it is face-center cubic structure (F.C.C) (JCPDS No. 04-0783). After the decoration CNTs with silver nanoparticles, the XRD pattern for MWCNTs/Ag NPs and SWCNTs/Ag NPs revealed two obvious diffraction peaks at  $2\theta=26.255^\circ$  which correspond with miller indices (002) for CNTs (MWCNTs & SWCNTs) and  $2\theta=44.143^\circ$  match with both miller indices (100) for CNTs and (200) for Ag NPs [14-16] as shown in (Fig.7 (b)).

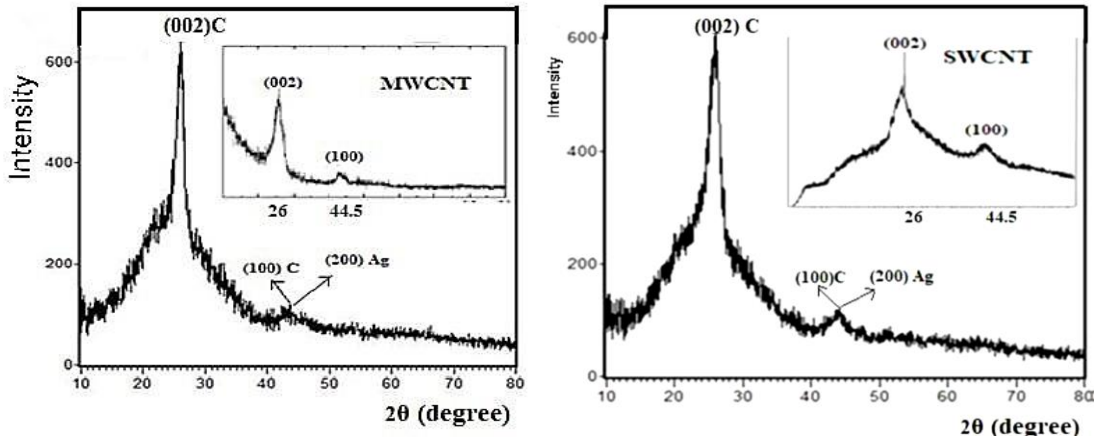


Figure 7b: XRD patterns (right) for SWCNTs/Ag NPs (left) for MWCNTs/Ag NPs thin film.

### 3.4. Field Emission- Scanning Electron Microscopy (FE-SEM)

From (Fig.8 (a)), the FESEM shows spherical clustered and luminous spots that correspond to the silver nanoparticles with the average particle size ranged between about (50-80 nm). The nanotubes were subsequently decorated with silver nanoparticles, (Fig.8 (b) shows the FESEM of the Ag NPs decorated MWCNTs and SWCNTs. The luminous particles on the CNT surfaces are the silver nanoparticles. The nanoparticles on the surface of the CNTs are equally distributed, and the density of the attached nanocrystals is high, as shown in the image. Because metal nanoparticles are easily agglomerated, NPs are conjugated with carbon nanotubes to overcome problems with NP stabilization, separation, and recovery, as well as to avoid NP aggregation [5].

### 3.5. Hall Effect measurement

The Hall Effect was used to study the electrical properties of CNTs/Ag NPs deposited on silicon (charge concentration, conductivity, carrier mobility, Hall coefficient and resistivity). The Hall measurements parameters for CNTs /Ag-NPs deposited on Si are exhibited in Table 1. Table 1 shows that the electric conductivity of CNTs/Ag NPs become much higher than that of Ag NPs and the concentration of carriers increased when CNTs were decorated with Ag NPs. Also, it can be seen that CNTs decorated with Ag NPs were converted from n-type to – p-type when Ag NPs were added to CNTs, which results in a shift in the Fermi energy from the valence band to mid-gap. The electrical transport of CNT/Ag NPs was improved when the CNTs were decorated with Ag NPs. And when CNTs/Ag NPs deposited on silicon substrates is p-type semiconductor, the mobility and conductivity have better values.

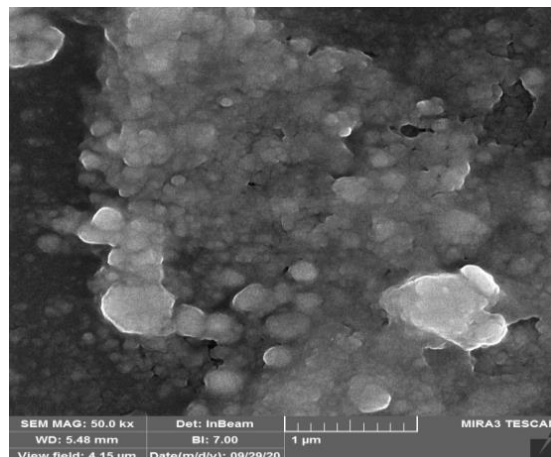


Figure 8a: FESEM image of pure Ag NPs.

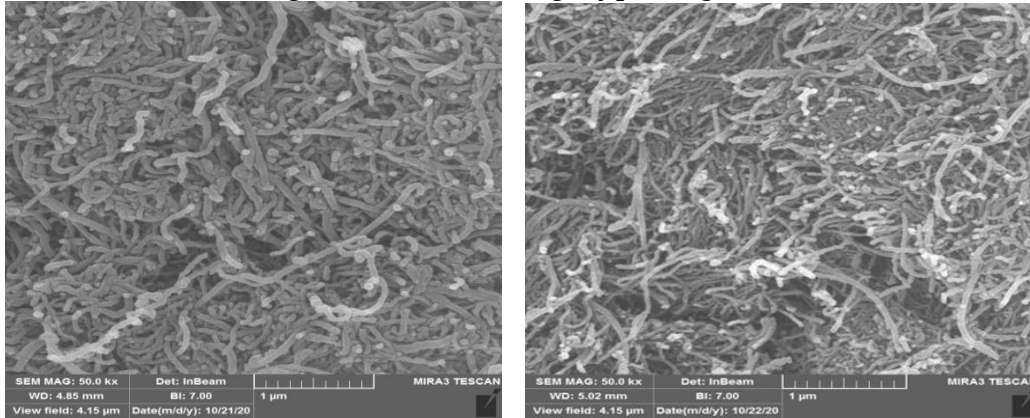


Figure 8b: FESEM images of SWCNTs/Ag NPs (right) and for MWCNTs/Ag NPs (left).

Table 1: Hall measurement parameters.

Parameter	Charge Concentration (1/cm <sup>3</sup> )	Conductivity (1/Ω.cm)	Mobility (Cm <sup>2</sup> /Vs)	Resistivity (Ω.cm)	Type
Ag NPs	-1.08×10 <sup>13</sup>	2.36×10 <sup>-1</sup>	1.36×10 <sup>5</sup>	4.23	N-type
MWCNTs/Ag NPs	1.80×10 <sup>22</sup>	8.83×10 <sup>4</sup>	3.07×10 <sup>1</sup>	1.132×10 <sup>-5</sup>	P-type
SWCNTs/Ag NPs	1.99×10 <sup>22</sup>	1.03×10 <sup>4</sup>	3.22	9.708×10 <sup>-5</sup>	P-type
MWCNTs/Ag NPs/Si	9.85×10 <sup>16</sup>	9.91	6.28×10 <sup>2</sup>	0.1	P-type

### 3.6. I-V Characteristics for photoconductive detector

The current-voltage characteristics (I-V characteristics) of the fabricated photoconductive detector are illustrated in (Fig.9) at forward bias voltage of (0.5-10) volt. The linear I-V curve indicates the ohmic nature of the detector. The photocurrent increased under illumination with a tungsten lamp of (250 W, 500-800 nm), ultra-violet light of (10W, 365nm) and infrared light of (300 mW, 808 nm). For polyamide nylon polymer coated films the results showed that the photocurrent of the polymer coating on CNTs/Ag NPs /Si layer samples are higher than without the polymer. This polymer coating can be considered as a surface treatment of the detector film, which highly increases the photoresponse and specific detectivity of the fabricated detector. The (I-V) characterization of the fabricated photoconductive detector on silicon layer with and without coated polymer are shown in Fig. 9 (a, b and c).

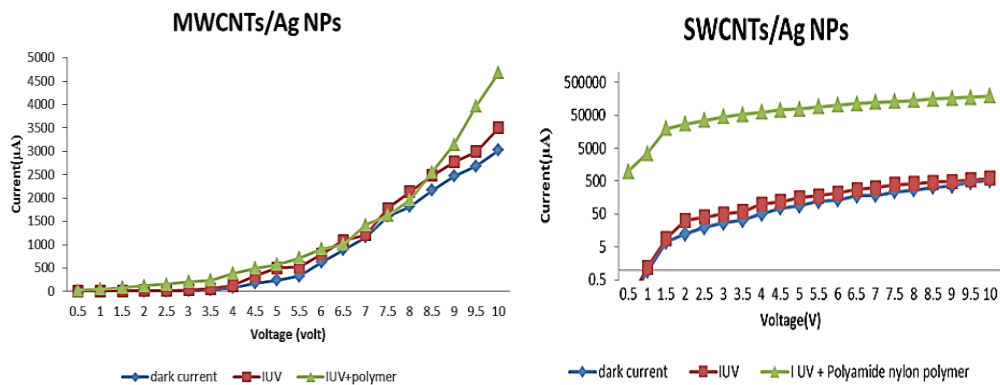


Figure 9a: The variation of the UV photo-current of the fabricated photoconductive detector with coating polymer for SWCNTs/Ag NPs and MWCNTs/Ag NPs.

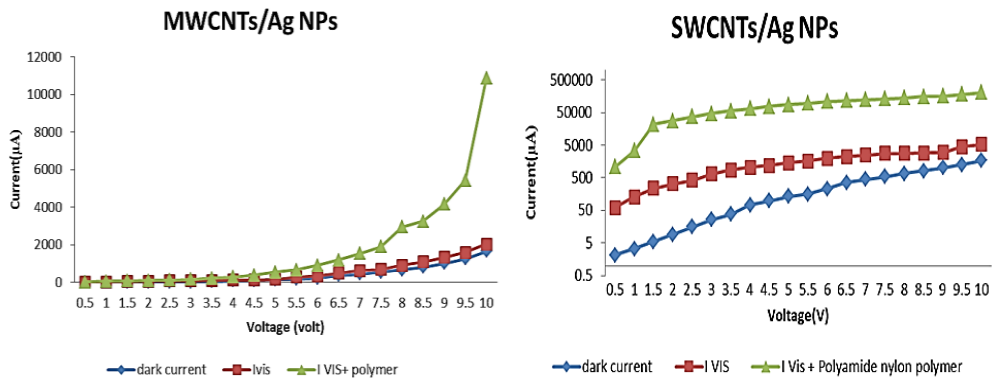


Figure 9b: The variation of the visible photo-current of the fabricated photoconductive detector with coating polymer for SWCNTs/Ag NPs and MWCNTs/Ag NPs.

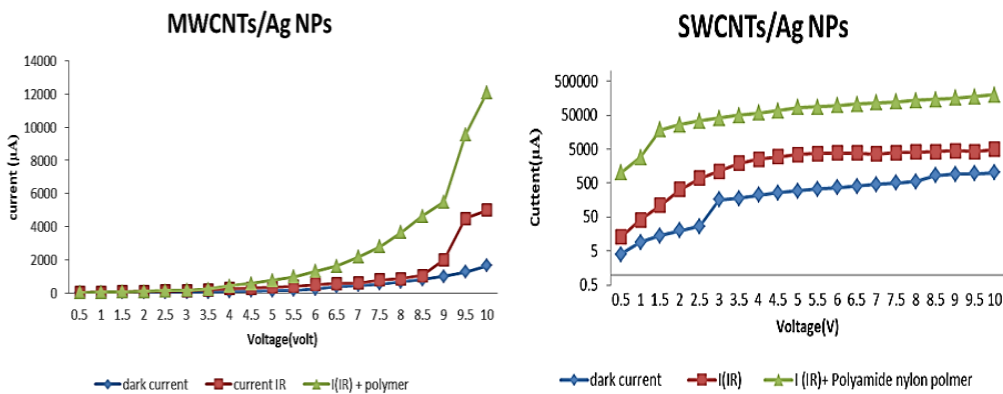


Figure 9c: The variation of the IR photo-current of the fabricated photoconductive detector with coating polymer for SWCNTs/Ag NPs and MWCNTs/Ag NPs.

Figure of merits of the coating polymer and of the photoconductive detector for different source of light (UV, Visible and IR) are shown in Table 2. The photocurrent gain (G) which is the ratio between the photocurrent and the dark current for the same bias voltage ( $G=I_{pb}/I_D$ ), responsivity ( $R_\lambda = I_{pb}/P_{in}$ ), noise equivalent power ( $NEP= I_n/R_\lambda$ ), Detectivity ( $D=1/NEP$ ) and specific detectivity ( $D^*=D(A \Delta f)^{1/2}$ ) were calculated. It can be observed from the results that the photocurrent of the polymer coating on SWCNTs/Ag NPs samples are higher than that of MWCNTs/Ag NPs in UV, Visible and IR radiation and have a good responsivity and photocurrent gain.

Table 2: Figure of merits photoconductive detector on silicon layer with coating polymer.

Sample	G	$R_\lambda$ (Amp/Watt)	NEP (Watt)	D (Watt <sup>-1</sup> )	D* (Watt <sup>-1</sup> . Hz <sup>1/2</sup> .cm)
<b>UV light</b>					
SWCNTs/Ag NPs	615	$8190 \times 10^{-6}$	0.019	52.6	52.6
MWCNTs/Ag NPs	2.6	$62.6 \times 10^{-6}$	4.5	0.22	0.22
<b>Tungsten lamp</b>					
SWCNTs/Ag NPs	654	$348 \times 10^{-6}$	0.06	16.6	16.6
MWCNTs/Ag NPs	4.2	$2.17 \times 10^{-6}$	95	0.01	0.01
<b>Laser diode (808nm)</b>					
SWCNTs/Ag NPs	640.6	$12200 \times 10^{-6}$	0.025	400	400
MWCNTs/Ag NPs	6	$1130 \times 10^{-6}$	0.18	5.5	5.5

#### 4. Conclusions

The wide band photoconductive detectors prepared by the drop casting technique on (p-type) silicon were fabricated and characterized to work in the UV, Vis. and IR regions. The decorating of CNTs (MWCNTs and SWCNTs) with silver nanoparticles synthesized by electro-exploding wire method was studied. It was found that the silver nanoparticles well dispersed on the surface of carbon nanotubes. The FTIR proved the interaction between CNTs and silver nanoparticles. The decorated of carbon nanotubes with Ag NPs significantly improved optical absorption of CNTs. CNTs / Ag NPs absorbed light in the 300-1000 nm range better than CNTs alone, demonstrating the importance of noble metals in CNT optical absorption. The nanoparticles on the surface of the CNTs are rather evenly dispersed, according to the FESEM image. From Hall measurements, it was found that the decorating CNT surface with Ag NPs changed its characteristics from n-type to p-type. The experimental results showed that the CNTs/Ag-NPs can become essential building blocks for photoconductive detector fabricated on (P-type) silicon. The coating of the films surfaces with a polyamide nylon polymer improved the photocurrent gain, photo-responsivity, and specific detectivity in both SWCNTs/Ag NPs and MWCNTs/Ag NPs detectors. The photocurrent gain for SWCNTs/Ag NPs with coating polymer in UV, Vis. and IR light was better than photocurrent gain for MWCNTs/Ag NPs with coating polymer.

#### Acknowledgments

The authors would like to thank department of physics, College of science, University of Baghdad to support this work.

#### Conflict of interest

Authors declare that they have no conflict of interest.

#### References

1. Elilarassi R., Maheshwari S., and Chandrasekaran G., *Structural and optical characterization of CdS nanoparticles synthesized using a simple chemical reaction route*. Optoelectron. Adv. Mater, 2010. **4**: pp. 309-312.
2. Hirlekar R., Yamagar M., Garse H., Vij M., and Kadam V., *Carbon nanotubes and its applications: a review*. Asian journal of pharmaceutical and clinical research, 2009. **2**(4): pp. 17-27.
3. Lanje A.S., Sharma S.J., and Pode R.B., *Magnetic and electrical properties of nickel nanoparticles prepared by hydrazine reduction method*. Arch Phys Res, 2010. **1**(1): pp. 49-56.
4. Travessa D.N., Silva F.S.d., Cristovan F.H., Jorge Jr A.M., and Cardoso K.R., *Ag ion decoration for surface modifications of multi-walled carbon nanotubes*. Materials Research, 2014. **17**(3): pp. 687-693.
5. Ahmed D.S., Mohammed M.R., and Mohammed M.K., *Synthesis of multi-walled carbon nanotubes decorated with ZnO/Ag nanoparticles by co-precipitation method*. Nanoscience & Nanotechnology-Asia, 2020. **10**(2): pp. 127-133.
6. He X., Léonard F., and Kono J., *Uncooled carbon nanotube photodetectors*. Advanced Optical Materials, 2015. **3**(8): pp. 989-1011.
7. Kruse P., Long D., Milton A., Putley E., Teich M., and Zwicker H., *Optical and infrared detectors*. Vol. 19. 1980: Springer.
8. Liu L. and Zhang Y., *Multi-wall carbon nanotube as a new infrared detected material*. Sensors and Actuators A: Physical, 2004. **116**(3): pp. 394-397.
9. Naje A.N. and Noori O., *A Carbon Nanotubes Photoconductive Detector in Near-Infrared Region*. IJAIEM, 2015. **4**: pp. 105-108.

10. Anouar M., Jbilat R., Le Borgne V., Ma D., and El Khakani M.A., *Ag nanoparticle-decorated single wall carbon nanotube films for photovoltaic applications*. Materials for Renewable and Sustainable Energy, 2016. **5**(1): pp. 1-9.
11. Lin Y., Watson K.A., Fallbach M.J., Ghose S., Smith Jr J.G., Delozier D.M., Cao W., Crooks R.E., and Connell J.W., *Rapid, solventless, bulk preparation of metal nanoparticle-decorated carbon nanotubes*. ACS nano, 2009. **3**(4): pp. 871-884.
12. Dinh N.X., Quy N.V., Huy T.Q., and Le A.-T., *Decoration of silver nanoparticles on multiwalled carbon nanotubes: antibacterial mechanism and ultrastructural analysis*. Journal of Nanomaterials, 2015. **16**(1): pp. 1-11.
13. Baudot C., Tan C.M., and Kong J.C., *FTIR spectroscopy as a tool for nano-material characterization*. Infrared Physics & Technology, 2010. **53**(6): pp. 434-438.
14. Hoyos-Palacio L.M., Castro D.P.C., Ortiz-Trujillo I.C., Palacio L.E.B., Upegui B.J.G., Mora N.J.E., and Cornelio J.A.C., *Compounds of carbon nanotubes decorated with silver nanoparticles via in-situ by chemical vapor deposition (CVD)*. Journal of Materials Research and Technology, 2019. **8**(6): pp. 5893-5898.
15. Choi S.K., Chun K.-Y., and Lee S.-B., *Selective decoration of silver nanoparticles on the defect sites of single-walled carbon nanotubes*. Diamond and related materials, 2009. **18**(4): pp. 637-641.
16. Yousif T.Y. and Naje A.N., *Characterization of carbon nanotube decorated silver nanoparticles*. Journal of Physics: Conference Series, 2021. **1879**(3): pp. 1-11.

## تعزير كاشف التوصيل الضوئي المعتمد على أنابيب الكربون النانوية المزينة بجسيمات الفضة النانوية عن طريق إضافة بوليمر موصل

تقوى يعرب يوسف، أسامة ناطق ناجي  
قسم الفيزياء، كلية العلوم، جامعة بغداد، بغداد، العراق

### الخلاصة

في هذا العمل ، تم تصنيع كاشف ضوئي واسع النطاق يعمل في نطاق الأشعة فوق البنفسجية والمرئية والأشعة تحت الحمراء باستخدام أنابيب الكربون النانوية (SWCNTs، MWCNTs) المزينة بجسيمات الفضة النانوية (Ag NPs). حيث تم استخدام السيليكون كركيزة لترسيب CNTs / Ag NPs عن طريق تقنية الصب النقطي. وتم طلاء بوليبيد نايلون بوليمر على CNT/Ag NPs لتعزير استجابة كاشف الضوئي. تم تحضير جسيمات الفضة النانوية باستخدام انفجار السلك الكهربائي . وتميزت الخصائص البصرية والتركيبية والكهربائية ل CNTs المزينة ب Ag NPs بحيود الأشعة السينية، والمجهر الإلكتروني لمسح الانبعثات الميدانية. اظهرت أنماط حيود الأشعة السينية من Ag NPs قيم  $\theta = (38.1^\circ, 44.3^\circ)$  المقابلة للبلورة النانوية الفضية، في حين أن نمط XRD من SWCNTs و MWCNTs / Ag NPs اظهرت قمم في  $\theta = 26.2^\circ$  والتي تتوافق مع (002) للكربون، و  $\theta = 44^\circ$  والتي تتوافق مع معاملات ميلر (100) للكربون و (200) للفضة النانوية. تم الكشف عن الخصائص البصرية التي تقاس بالتنظير الطيفي المرئي للأشعة فوق البنفسجية ، وتم تحسس ذروة الرنين السطحي العريض والقوي (SPR) عند 420 نانومتر، بالنسبة ل Ag NPs في حين ازداد امتصاص CNTs / Ag NPs بشكل كبير من الأشعة فوق البنفسجية إلى منطقة الأشعة تحت الحمراء القريبة (300-1000 نانومتر). يظهر تحليل المجهر الإلكتروني للمسح الميداني أن الأنابيب الكربون النانوية مزينة بالجسيمات النانوية الفضية دون أي شوائب، مع متوسط حجم الجسيمات حوالي (50-80) nm ل Ag-NPs، و (44-30) nm ل MWCNTs / Ag-NPs و (30-10) nm ل SWCNTs / Ag NPs. فرق الجهد المسلط عند قياس خصائص I-V كان (0.5-10) فولت. تم قياس مزايا الكاشف بعد طلاء البوليمر (الاستجابية، ربح التيار الضوئي، NEP) في الظلام وبعد الإضاءة بضوء الأشعة فوق البنفسجية (UV LED) (365 nm)، مصباح التتسكن (500-800 nm) ودايود الليزر (808 nm).